MECHANICAL PROPERTIES OF CFRP/TI-ALLOY LAMINATED COMPOSITES

Norio Arai*, Toshio Ogasawara, Tomohiro Yokozeki**, Takeshi Ogawa***
***Aoyamagakuin University, ** Japan Aerospace Exploration Agency**

Keywords: *Polymer-matrix composites, Titanium alloy, Fiber metal laminated composites, transverse crack*

Abstract

In this paper, the mechanical behaviors of pure Ti and new β-Ti alloy films and CFRP/Ti-alloy laminated composites are investigated in order to research of development of fiber metal laminates tanks for cryogenic rocket propellants. Tensile tests of pure Ti and new β-Ti alloy films and CFRP/Ti-alloy laminated composites are performed. Characterization of the nonlinear behaviors of pure Ti and new β-Ti alloy films are evaluated by elastoplastic model. As for CFRP/β-Ti alloy, it is shown that there is little residual strain compared with CFRP/pure Ti. Internal damage is evaluated by cross-sectional observation. From the cross-sectional observation, no damage was observed in the metal layer, though transverse cracks were propagated in the CFRP 90 ° layers.

1 Introduction

Carbon fiber reinforced plastic (CFRP) are attractive structural materials in aerospace structures because of high specific stiffness and strength. To achieve radical structural weight reduction of space launch vehicle, application of CFRP laminates to the cryogenic propellant tank (e.g. liquid hydrogen liquid oxygen tanks) has been widely attempted. Some recent studies of the feasibility of composite cryogenic propellant tank indicate that matrix crack onset and its accumulation are inevitable because of severe thermomechanical loads when applying conventional high performance composites to cryogenic tanks. Those accumulated multilayer matrix cracks might engender detrimental propellant leakage, as shown Fig.1. Therefore, fuel leakage or gas leakage through a damage network in CFRP laminates turned out to be a major problem that dominates the feasibility of composite cryogenic propellant tanks. Adequate guidelines for reliable application of CFRP laminates to cryogenic propellant tanks are necessary from both leakage and damage tolerance perspectives.

Yokozeki et al. curried out experimental measurement of gas leakage through damaged CFRP laminates using $[0_2/\theta_2]s$ (θ=45, 60, 75 and 90) coupon specimens to assess the effect of crack intersecting angle on the leakage [1]. Their results indicated correlation between uniaxial loadings and gas leak rates. Moreover, the leakage conductance was evaluated by using the semi-analytical leakage model based on the leak conductance of crack intersections.

To prevent cryogenic composite tanks from propellant leaks due to microscopic damages, metal lined cryogenic composite tanks have been developed [2]. However, because of significant thermal expansion mismatch between CFRP and liner materials, the technology has not been established.

By the way, hybrid laminates such as ARALL

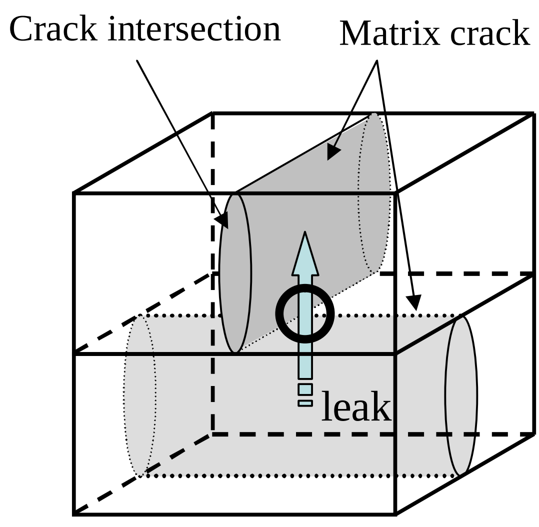

Fig. 1. Leak path induced by multilayer matrix crack

(aramid fiber / aluminium laminates), GLARE (Glass fiber / aluminium laminates), and TiGr (Graphite (carbon) fiber / Titanium laminates), sometimes called fiber metal laminates (FML), are made of polymer matrix composites (PMC) plies interspersed with plies of metal film. The two materials are assembled by bonding the PMC plies and metal film to form a composites laminate [3]. The most important benefit of FML is improvement of fatigue resistance. For example, it is reported that ARALL provides up to 15-20 % lower density and up to 60% higher fatigue strength than monolithic aluminum alloy [4]. ARALL and GLARE have been applied for commercial aircrafts such as Fokker F-27, Boeing C-17, Airbus A-380 and others.

This study investigates the possibility of FML for gas barrier function. Objective of metal film insert is to improve gas barrier property, therefore only one metal layer was adopted. It is known that aluminium alloy is inadequate for carbon fiber composites because of Galvanic corrosion issue, therefore pure titanium and β-titanium alloy were applied. Stress/strain response and behaviours of matrix crack propagation are evaluated.

2 Experiment

2.1 Material

CFRP used in this study was IM600/#133 (Toho Tenax, Japan). The composite laminates were fabricated from unidirectional prepreg tapes having a thickness of 0.135 mm. The nominal fiber volume fraction was 55 %. Mechanical properties of IM600/#133 are listed in Table 1 [5,6]. Two kinds of cold-rolled titanium films, pure titanium (ASTM G1 grade) and β-titanium alloy (Ti-36Nb-2Ta-3Zr-0.3O, Toyotsu Material Co. Ltd. Japan) [7], were prepared. Thickness of each titanium film was 0.1 mm.

The β-titanium alloy (called as Gummetal™, and denoted as GM in this paper) used in this study was recently developed by Saito et al. of Toyota Central Research Institute. This titanium alloy has a super-elasticity such as low Young's modulus and high elastic deformation capability (up to 2.5%), compared to the conventional β-Ti such as Ti-15V-3Cr-3Sn-3Al [7]. Additionally, it is reported that the wire rod of this alloy has an Elinvar behavior with a small temperature dependency, a low CTE from cryogenic (-196℃) to high temperature (300℃), and excellent cold rolling processability.

CFRP/Ti laminated composites were made by inserting a titanium film (pure Ti or GM) in the center of a CFRP laminate without adhesive. The materials were cured using a hot press under a maximum pressure of 0.5 MPa and a curing temperature of 180 ºC. The stacking sequence was $[0]_2/[90]_2/Ti/[90]_2/[0]_2$. The resulting composite laminate has 1.18 mm of thickness, and 8.5 % of the volume fraction of Ti layer.

2.2 Experimental procedure

Monotonic and loading-unloading tensile behaviors were evaluated for pure Ti and GM. Loading-unloading tensile tests were conducted by repeating load and unload while increasing the strain given to the specimen by 0.3 %. Dog-bone shaped specimens having 124 mm length and 20 mm width were prepared for rolling and transverse directions, as shown Fig.3. A non-contact type optical extensometer was used for strain measurement.

Tensile test was also performed for CFRP/Ti composites and CFRP ($[0_2/90_2]_S$) under a constant displacement rate of 0.5 mm/min. The specimen has 190 mm length and 10 mm width, as shown Fig.4. A contact type extensometer (GL=25 mm) was used for measuring the strain. Microscopic damages were observed using an optical microscope.

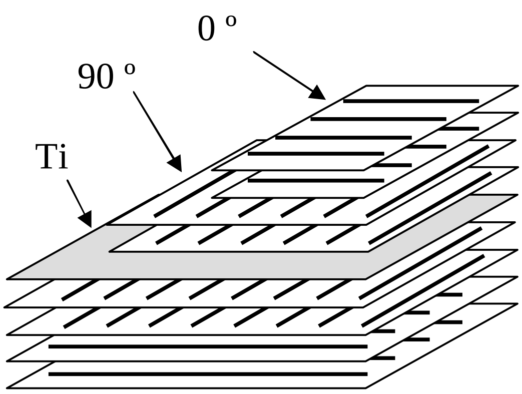

Fig. 2. Stacking sequence of CFRP/Ti composites

Table 1. Mechanical properties of IM600/#133

E_L [GPa]*	E_T [GPa]*	ν_{LT}*	G_{LT} [GPa]*	G_{TT} [GPa]**	α_L [10^{-6}/ºC]**	α_T [10^{-6}/ºC]**
153.0	8.2	0.335	3.98	7.1	-0.51	34.0

*[5], **[6]

3 Results and discussions

3.1 Tensile properties of pure Ti and GM

Fig.5 shows the stress/strain curve of pure Ti. The Young's modulus of the transverse direction is higher than the rolling direction. Fig.6 (a) and (b) show the stress/strain curves of GM. The Young's modulus of the transverse direction is higher than that of the rolling direction, similar to pure Ti. Nonlinear elastic behavior is clearly observed above 0.6 % of the strain. Hysteresis behavior is slightly observed in the stress/strain curves of GM.

Tensile strength, yield strain and the initial Young's modulus are summarized in Table 2. Young's modulus was calculated between 0.1 % and 0.3 % of strain. The GM has more than three times the tensile strength as compared with pure Ti. On the other hand, the Young's modulus of the GM is almost same as that of pure Ti. The yield strain of the GM is about 1.2 %, while that of pure Ti is about 0.4 %.

In this study, the modified elasticity model is applied for the description of nonlinear elastic behavior of GM. According to Hahn and Tsai [8], complementary energy of orthotropic materials for plane stress of forth-order are determine by

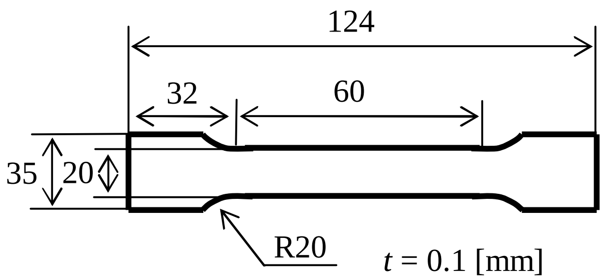

Fig. 3 Test specimen for tensile and loading-unloading test of pure titanium and new β-titanium alloy

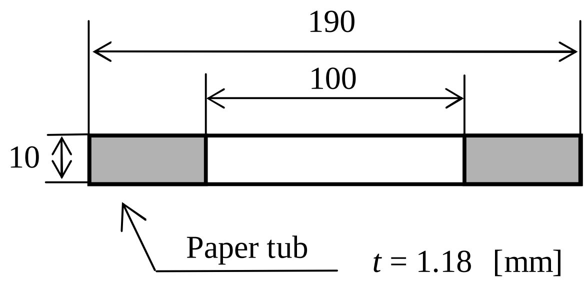

Fig. 4 Test specimen for tensile test of CFRP/Ti composites and CFRP ($[0_2/90_2]_S$)

$$\begin{aligned} W_C = &\frac{1}{2}S_{11}\sigma_1^{\,2} + \frac{1}{2}S_{22}\sigma_2^{\,2} + \frac{1}{2}S_{66}\sigma_6^{\,2} + S_{12}\sigma_1\sigma_2 \\ &+ \frac{1}{3}S_{111}\sigma_1^{\,3} + \frac{1}{3}S_{222}\sigma_2^{\,3} \\ &+ \frac{1}{4}S_{1111}\sigma_1^{\,4} + \frac{1}{4}S_{2222}\sigma_2^{\,4} + \frac{1}{4}S_{6666}\sigma_6^{\,4} \end{aligned} \tag{1}$$

where

$$\varepsilon_{ij} = \frac{\partial W_C}{\partial \sigma_{ij}} \tag{2}$$

Therefore, the elasticity strain-stress relations are shown Eq. (3).

$$\begin{aligned} \varepsilon_1 &= S_{11}\sigma_1^{\,2} + S_{111}\sigma_1^{\,3} + S^{1111}\sigma_1^{\,4} \\ \varepsilon_2 &= S_{22}\sigma_2^{\,2} + S_{222}\sigma_2^{\,3} + S_{2222}\sigma_2^{\,4} \end{aligned} \tag{3}$$

Eq. (4) is obtained from Eq. (3).

$$\begin{aligned} E_L &= 1/\left(S_{11} + S_{111}\sigma_1 + S_{1111}\sigma_1^{\,2}\right) \\ E_T &= 1/\left(S_{22} + S_{222}\sigma_2 + S_{2222}\sigma_2^{\,2}\right) \end{aligned} \tag{4}$$

Moreover, the modified plasticity model is applied for the description of orthotropic plastic behavior of pure Ti and GM. According to Hill [9], the plasticity potential is shown Eq (5).

$$\begin{aligned} 2f(\sigma_{ij}) \equiv &F(\sigma_2-\sigma_3)^2 + G(\sigma_3-\sigma_1)^2 + H(\sigma_1-\sigma_2)^2 \\ &+2L\tau_{23}^{\,2} + 2M\tau_{31}^{\,2} + 2N\tau_{12}^{\,2} \end{aligned} \tag{5}$$

The effective stress and the effective plastic strain are expressed as the Eq. (6) (7) when subjected to uniaxial loading with off-axis angle θ to the longitudinal axis (1 direction) [10].

$$\begin{aligned} \bar{\sigma} &= \sigma_x\sqrt{\frac{3}{2}\left(\cos^4\theta + a_{22}\sin^4\theta + (a_{66}-1)\cos^2\theta\sin^2\theta\right)} \\ &\equiv \sigma_x h(\theta) \end{aligned} \tag{6}$$

$$d\bar{\varepsilon}^{\,p} = \frac{d\varepsilon_x^{\,p}}{h(\theta)}, \quad \bar{\varepsilon}^{\,p} = \frac{\varepsilon_x^{\,p}}{h(\theta)} \tag{7}$$

Especially, uniaxial tension of 1 and 2 direction are expressed as

$$\begin{aligned} \bar{\sigma} &= \sqrt{\frac{3}{2}}\sigma_x, \quad & \bar{\varepsilon}^{\,p} &= \sqrt{\frac{2}{3}}\varepsilon_x^{\,p} \\ \bar{\sigma} &= \sqrt{\frac{3}{2}a_{22}}\sigma_x, \quad & \bar{\varepsilon}^{\,p} &= \sqrt{\frac{2}{3a_{22}}}\varepsilon_x^{\,p} \end{aligned} \tag{8}$$

Therefore, the effective stress and effective plastic strain can be expressed simply in term of experimental values in uniaxial tensile tests. The effective stress-effective plastic strain relation depends on the choice of a_{22} and a_{66}. The effective stress-effective plastic strain relation is approximated by Eq. (9).

$$\bar{\sigma} = A \cdot Ln\left(\bar{\varepsilon}^{p}\right) + B \qquad (9)$$

The obtained parameters are summarized in Table 4.

The stress-strain curves using the obtained parameters are compared with the experimental data (Fig.7). The analytical results agree with the experiment results. It is shown that the nonlinear elastic and plastic response of orthotropic metal film under tension load can be described using there parameters.

Table 2 Mechanical properties of Ti and GM

	Pure Ti		GM	
	Rolling	Transverse	Rolling	Transverse
E_x [GPa]	74.7	109.9	72.0	80.0
σ_B [MPa]	316.0	302.9	1070.1	1117.7
$\sigma_{0.2}$ [MPa]	187	225	741 ~ 863	860 ~ 989
ε_Y [%]	0.471	0.498	1.2~1.5	1.2~1.5

Table 3 Nonlinear elastic parameters of GM

	S_{11} [1/GPa]	S_{111} [1/GPa^2]	S_{1111} [1/GPa^3]
Rolling	$1.51\text{x}10^{-03}$	$-4.27\text{x}10^{-08}$	$4.08\text{x}10^{-10}$
Transverse	$1.15\text{x}10^{-03}$	$7.60\text{x}10^{-08}$	$2.48\text{x}10^{-10}$

Table 4 Orthotropic plastic parameters of pure Ti and GM

	α_{22}	A [MPa]	B [MPa]
Pure Ti	0.97	37.4	188.5
GM	0.93	58.1	362.6

3.2 Tensile properties of CFRP/Ti and CFRP/GM

Fig.8 shows stress/strain curves of CFRP/Ti, CFRP/GM and CFRP. Delamination at the interface between CFRP and Ti layer was not observed before the final fracture during tensile tests. Increase in stiffness with increasing stress is observed in the stress/strain curves of all the materials. This is due to nonlinear elastic behavior of carbon fiber [11]. For CFRP/GM, the slight decrease in stiffness was observed above 1.0 % of strain compared with other materials.

Mechanical properties of CFRP, CFRP/Ti, and CFRP/GM are summarized in Table 5. The tensile strength, fracture strain, and Young's modulus of CFRP/Ti and CFRP/GM were almost the same as those of CFRP. The influence of Ti film insert on tensile strength and stiffness is not considerable. The Young's modulus values calculated from classical lamination theory are also listed in Table 5. The calculated values are almost the same as the experimental results. The discrepancy between calculated and experimental results is probably due to the difference in the fiber volume fraction.

Fig.9 shows stress/strain curves obtained from the loading-unloading tensile tests of CFRP/Ti and CFRP/GM. For CFRP/Ti, the residual strain at zero stress appears above 0.3 % of the strain. On the other hand, onset of residual strain for CFRP/GM is above 1.2 %. Fig.7 indicates that the onset strain of plastic deformation is about 0.3 % and 1.2 % for Ti and GM, respectively. Therefore, the residual strain observed in the CFRP/Ti laminates is mainly caused by the plastic deformation of an inserted titanium layer.

Microscopic damages were observed for the CFRP/Ti and CFRP/GM specimens subjected to 1.3 % of tensile strain. Fig.10 (a) and (b) show optical micrographs illustrating cross-sections of the CFRP/Ti and CFRP/GM. Transverse cracks propagated in 90 ° layers were observed, while fiber breakage and delamination at the interface between CFRP and Ti layer were not observed. The transverse cracks in 90° layer are arrested at the surface of a Ti layer, and no microscopic damage was observed in the inserted Ti layer. A number of transverse cracks were counted, consequently the transverse crack density was 4.0 cm^{-1} for CFRP/Ti, and 9.8 cm^{-1} for CFRP/GM. CFRP/GM has about 2.5 times of crack density as compared with CFRP/Ti. It is known that the stiffness of composite laminates decreases with transverse crack density. [12] The transverse crack density of CFRP/GM is higher than that of CFRP/Ti. Therefore, it is suggested that the stiffness decrease of CFRP/GM in Fig.8 was mainly caused by an accumulation of transverse cracks. Experimental and analytical studies will be made to understand the effect of Ti layer insert on transverse crack propagation behavior.

In this study, it was revealed that transverse cracks in CFRP do not propagate in Ti layer, and no delamination at the interface between CFRP and the Ti layer occurs before the final fracture. The experiment results suggest that this material have some gas barrier

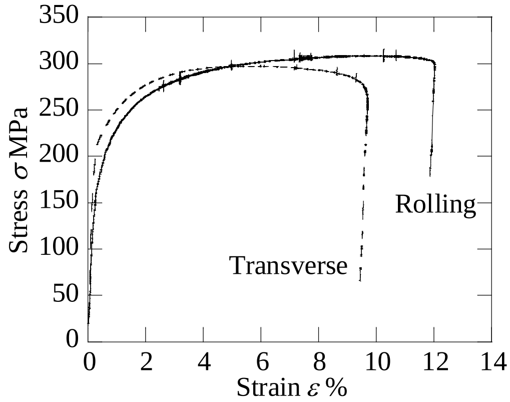

Fig. 5. Stress/strain curves of pure Ti

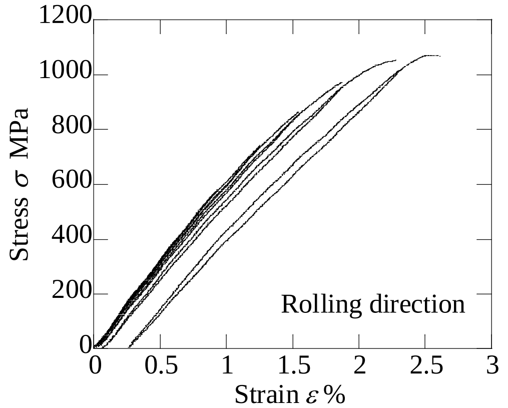

(a) Rolling direction

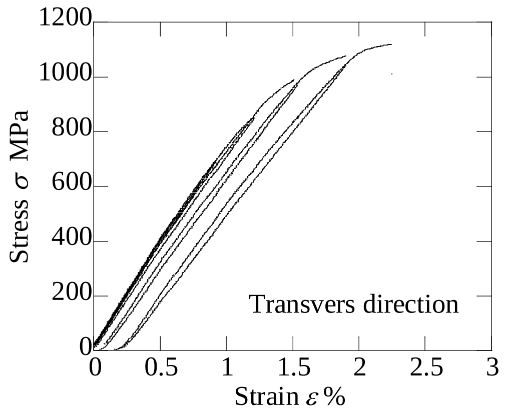

(b) Transverse direction

Fig. 6. Stress/strain curves of GM

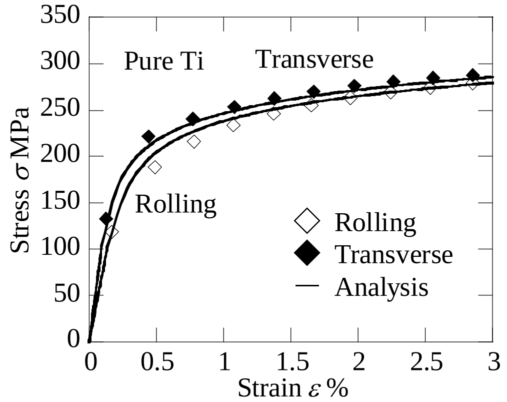

(a) Pure Ti

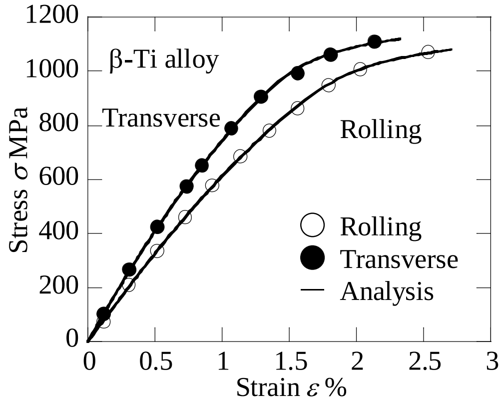

(b) GM

Fig. 7. Comparison of experimental and analytical stress/strain curves

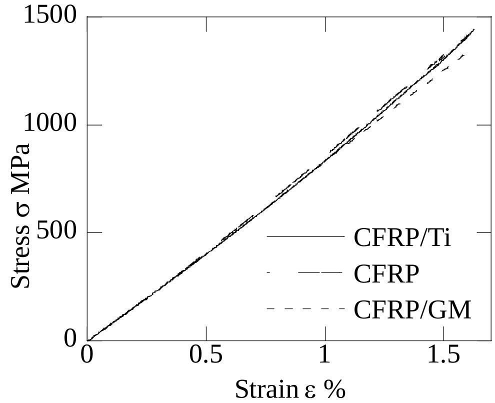

Fig. 8. Stress/strain curves obtained by the tensile tests of CFRP/Ti, CFRP/GM and CFRP

Table 5 Mechanical properties of CFRP, CFRP/Ti and CFRP/GM

	E_x (measured) [GPa]	E_x (theoretical) [GPa]	σ_B [MPa]	ε_F [%]
CFRP	80.4	83.1	1424	1.59
CFRP/Ti	80.3	83.8	1563	1.75
CFRP/GM	82.4	83.6	1455	1.64

* Young's modulus was calculated between 0.1 % and 0.3 % of strain.

capability. Evaluation of mechanical properties, durability under thermal cycle and helium gas leak behavior will be examined under cryogenic temperature (liquid nitrogen and liquid helium) as well as room temperature.

This composite material has weak point in case of making large components. This is existence of discontinuity of a metal layer at the abutting edges of prepregs. The discontinuous parts become the gas leak pass as shown in Fig. 1. From this viewpoint, experimental and analytical studies should be carried out.

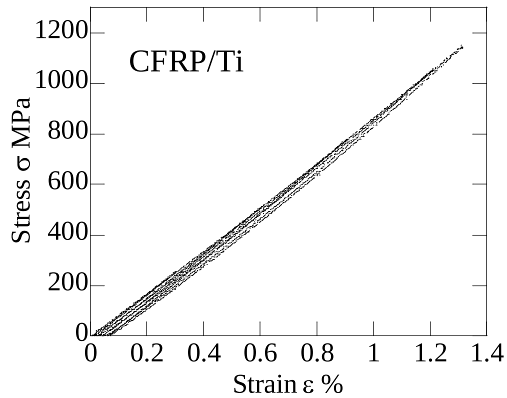

(a) CFRP/Ti

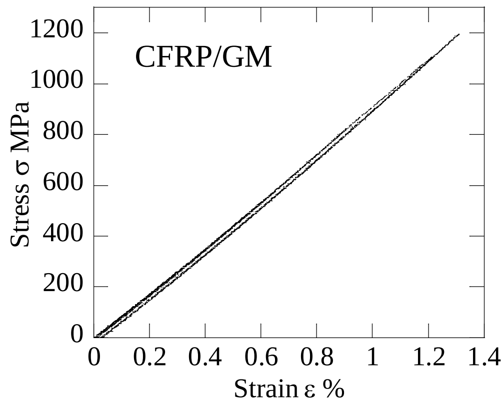

(b) CFRP/GM

Fig. 9. stress/strain curves obtained by the loading-unloading test of CFRP/Ti and CFRP/GM

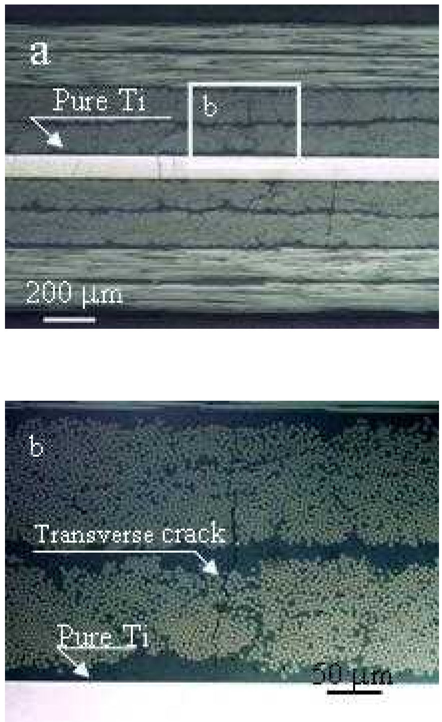

(a) CFRP/Ti

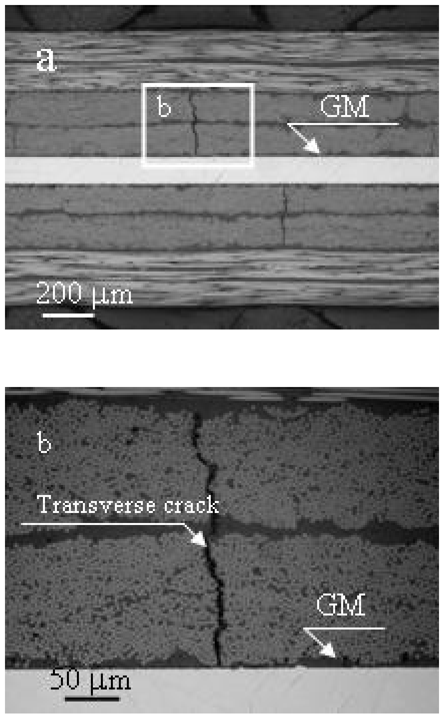

(b) CFRP/GM

Fig.10. Cross-section of CFRP/Ti and CFRP/GM after tensile test (strain 1.3 %)

4 Conclusions

This study investigates the possibility of fiber/metal laminated composites for gas barrier function. The following conclusions were made;

1. The tensile strength and yield strain of the new β-Ti alloy (Gummetal^{TM}) were three times higher as compared with those of pure Ti.
2. Elastic/plastic constituent model was proposed to evaluate the nonlinear behaviors of pure Ti and new b-Ti alloy films.
3. Ultimate tensile strength and Young's modulus of CFRP/Ti and CFRP/β-Ti alloy were almost the same as those of CFRP.
4. The residual onset strain of CFRP/GM after unloading was about 1.2 % of strain, whereas that of CFRP/Ti was 0.3 %.
5. No damage was observed in the metal layer after tensile test for CFRP/Ti and CFRP/β-Ti alloy, although the transverse cracks were propagated in CFRP 90 ° layers.

References

[1] Yokozeki T., Ogasawara T., Ishikawa T. Evaluation of gas leakage through composites with multilayer cracks: Cracking angle effect, Composites Science and Technology, Vol.66, pp.2815-2824, 2006

[2] Y. Torano, M. Arita, H. Takahashi. Current Study Status of the Advanced Technologies for the J-1 Upgrade Launch Vehicle -Cryogenic Composite Tank-, AIAA paper 2001-1877

[3] Dennis A., S. Mark. Delamination growth from face sheet seams in cross-ply titanium/graphite hybrid laminates, Composites Science and Technology, Vol.61, pp.261-269, 2001

[4] Wilson CD, Wilson DA. Effective crack lengths by compliance measurement for ARALL-2 laminates. Composite Materials: Fatigue and Fracture, ASTM STP 1110, pp791-805, 1991

[5] Advanced Composites Database System: JAXA-ACDB; Ver.06-1, http://www.jaxa-acdb.com/

[6] Aoki T, Ishikawa T, Kumazawa H, Morino Y. Mechanical performance of CF/polymer composite laminates under cryogenic conditions, AIAA paper 2000-1605

[7] Saito T. et al., Multifunction Alloys Obtained via a Dislocation-Free Plastic Deformation Mechanism, Science, Vol.300, pp.464-467, 2003

[8] T. Hahn and S. W. Tsai, Nonlinear Elastic Behavior of Unidirectional Composite Lamina, Journal of Composite Materials, Vol.7, pp.102-118, 1973

[9] Hill. R. The Mathematical Theory of Plasticity, Oxford University Press, London, 1950

[10] C. T. Sun and J. L. Chen. A Simple Flow Rule for Characterizing Nonlinear Behavior of Fiber Composites, J. Comp. Mater., Vol.23, pp.1009-1020, 1989

[11] Yokozeki, T., Ogasawara T., Ishikawa, T., “Nonlinear behavior and compressive strength of unidirectional and multidirectional carbon fiber composite laminates”, Composites. Part A, vol. 37, pp2069-2079, 2006

[12] Whitney J. M., Effective elstic constants of bidirectional laminates containing transverse ply cracks, J. Comp. Mater., 34, pp 954-78 2003